Inorg. Chem. **2005**, *44*, 8116–8124

Synthesis and Reactivity of $W_3Te_7^{4+}$ Clusters and Chalcogen Exchange in the M_3Q_7 (M = Mo, W; Q = S, Se, Te) Cluster Family

Maxim N. Sokolov,*,† Pavel A. Abramov,† Artem L. Gushchin,† Irina V. Kalinina,† Dmitry Y. Naumov,† Alexander V. Virovets,† Eugenia V. Peresypkina,† Cristian Vicent,‡ Rosa Llusar,‡ and Vladimir P. Fedin†

Nikolayev Institute of Inorganic Chemistry, Siberian Branch of the Russian Academy of Sciences, Lavrentiev Avenue 3, Novosibirsk 630090, Russia, and Departament de Ciencies Experimentals, Universitat Jaume I, Castellon, Spain

Received June 14, 2005

Heating WTe_2, Te, and Br_2 at 390 °C followed by extraction with KCN gives $[W_3Te_7(CN)_6]^{2-}$. Crystal structures of double salts $Cs_{3.5}K\{[W_3Te_7(CN)_6]Br\}Br_{1.5}\cdot 4.5H_2O$ (**1**), $Cs_2K_4\{[W_3Te_7(CN)_6]_2Cl\}Cl\cdot 5H_2O$ (**2**), and $(Ph_4P)_3\{[W_3Te_7(CN)_6]Br\}\cdot H_2O$ (**3**) reveal short $Te_2\cdots X$ (X = Cl, Br) contacts. Reaction of polymeric $Mo_3Se_7Br_4$ with KNCSe melt gives $[Mo_3Se_7(CN)_6]^{2-}$. Reactions of polymeric $Mo_3S_7Br_4$ and $Mo_3Te_7I_4$ with KNCSe melt (200–220 °C) all give as final product $[Mo_3Se_7(CN)_6]^{2-}$ via intermediate formation of $[Mo_3S_4Se_3(CN)_6]^{2-}/[Mo_3SSe_6(CN)_6]^{2-}$ and of $[Mo_3Te_4Se_3(CN)_6]^{2-}$, respectively, as was shown by ESI-MS. $(NH_4)_{1.5}K_3\{[Mo_3Se_7(CN)_6]I\}I_{1.5}\cdot 4.5H_2O$ (**4**) was isolated and structurally characterized. Reactions of $W_3Q_7Br_4$ (Q = S, Se) with KNCSe lead to $[W_3Q_4(CN)_9]^{5-}$. Heating $W_3Te_7Br_4$ in KCNSe melt gives a complicated mixture of W_3Q_7 and W_3Q_4 derivatives, as was shown by ESI-MS, from which $\hat{E}_3[W_3(\mu_3\text{-Te})(\mu\text{-TeSe})_3(CN)_6]Br\cdot 6H_2O$ (**5**) and $K_5[W_3(\mu_3\text{-Te})(\mu\text{-Se})_3(CN)_9]$ (**6**) were isolated. X-ray analysis of **5** reveals the presence of a new $TeSe^{2-}$ ligand. The complexes were characterized by IR, Raman, electronic, and ^{77}Se and ^{125}Te NMR spectra and by ESI mass spectrometry.

Introduction

Metal telluride clusters remain the least studied members of the chalcogenide cluster family.[1−6] The large size, diffuse orbitals, and increased metallic character of tellurium make it an attractive cluster-supporting bridging ligand, often with a quite different behavior, in comparison with a rather sulfur-like selenium.[7] A strong tendency of tellurium to participate in secondary nonvalence intermolecular interactions, already observable in elemental Te, makes a strong case for using tellurium-containing building blocks in supramolecular chemistry.[8] On the other hand, the M−Te bonds are weak and one can expect an easy replacement of Te by other bridging ligands with the cluster core retention. Cluster cyanides have drawn much attention in recent years as building blocks for coordination polymers, in particular for those with large cavities and high porosity. Both tetrahedral $\{M_4Q_4(CN)_{12}\}$ and octahedral $\{M_6Q_8(CN)_6\}$ (M = Mo, W, Re; Q = S, Se, Te) units were used for these purposes.[9,10] In this contribution we report the synthesis and structures of new trinuclear chalcogenide cluster cyanides, $[W_3Te_7(CN)_6]^{2-}$ and $[Mo_3Se_7(CN)_6]^{2-}$, as well as the use of KNCSe melt for introduction of Se into cluster cores with the retention of the metal framework, which allows one to obtain new mixed Se/Te clusters $[W_3Te_4Se_3(CN)_6]^{2-}$ and $[W_3TeSe_3(CN)_9]^{5-}$.

* To whom correspondence should be addressed. E-mail: caesar@che.nsk.su.

† Siberian Branch of the Russian Academy of Sciences.

‡ Universitat Jaume I.

(1) Kolis, J. W. *Coord. Chem. Rev.* **1990**, *105*, 195.
(2) Roof, L. C.; Kolis, J. W. *Chem. Rev.* **1993**, *93*, 1037.
(3) Fenske, D.; Corrigan, J. F. In *Metal Clusters in Chemistry*; Braunstein, P., Oro, L. A., Raithby, P. R., Eds.; Wiley-VCH: Weinheim, Germany, 1999; Vol. 3, p 1303.
(4) Kalinina, I. V.; Fedin, V. P. *Russ. J. Coord. Chem.* **2003**, *29*, 597.
(5) Sokolov, M. N.; Fedin, V. P.; Sykes, A. G. *Comp. Coord. Chem. 2* **2003**, *4*, 761.
(6) Sokolov, M. N.; Fedin, V. P. *Coord. Chem. Rev.* **2004**, *248*, 925.
(7) Wachter, J. *Eur. J. Inorg. Chem.* **2004**, 1367.
(8) Smith, D. M.; Ibers, J. A. *Coord. Chem. Rev.* **2000**, *200−202*, 187.
(9) (a) Fedin, V. P.; Virovets, A. V.; Kalinina, I. V.; Ikorskii, V. N.; Elsegood, M. R. J.; Clegg, W. *Eur. J. Inorg. Chem.* **2000**, 2341. (b) Fedin, V.; Kalinina, I.; Gerasimenko, A.; Virovets, A. *Inorg. Chim. Acta* **2002**, *331*, 48. (c) Kalinina, I. V.; Virovets, A. V.; Dolgushin, F. M.; Antipin, M. Yu.; Llusar, R.; Fedin, V. P. *Inorg. Chim. Acta* **2004**, *357*, 3390. (d) Fedin, V. P.; Kalinina, I. V.; Virovets, A. V.; Fenske, D. *Russ. Chem. Bull., Int. Ed.* **2003**, *52*, 126.
(10) (a) Brylev, K. A.; Sekar, P.; Naumov, N. G.; Fedorov, V. E.; Ibers, J. *Inorg. Chim. Acta* **2004**, *357*, 738. (b) Mironov, Y. V.; Fedorov, V. E.; Ijjaali, I.; Ibers, J. A. *Inorg. Chem.* **2001**, *40*, 6320.

10.1021/ic050962c CCC: $30.25
Published on Web 09/27/2005

Experimental Section

Materials and Methods. $Mo_3Te_7I_4$ and the bromides $M_3Q_7Br_4$ (M = Mo, W; Q = S, Se) were prepared by heating stoichiometrical mixtures of elements (350 °C, 4 days) according to the published procedure.[11,12] WTe_2 was prepared from the elements.[13] All the other reagents were purchased from commercial sources and used without further purification. Hygroscopic KNCSe (Aldrich) was used immediately after opening and kept over P_4O_{10}. The reactions with KNCSe were run under argon, and all the other manipulations were done in air.

Elemental analyses were carried out by the Novosibirsk Institute of Organic Chemistry microanalytical service. IR spectra (4000−400 cm^{-1}) were recorded on an IFS-85 Fourier spectrometer (Bruker). Raman spectra were obtained on a Triplimate SPEX spectrometer using the 632.8 nm line of a He−Ne laser for excitation. ^{77}Se NMR and ^{125}Te NMR spectra were run on a SXP/300 spectrometer (Bruker) with saturated aqueous solutions of H_2SeO_3 and H_6TeO_6 as standards. The chemical shifts for ^{77}Se spectra were recalculated vs Me_2Se. A Quattro LC (quadrupole−hexapole−quadrupole) mass spectrometer with an orthogonal Z-spray−electrospray interface (Micromass, Manchester, U.K.) was used. The drying gas as well as nebulizing gas was nitrogen at a flow rate of 400 and 80 L/h, respectively. Sample solutions in methanol were infused via syringe pump directly to the interface at a flow rate of 6 μL/min. A capillary voltage of 3.5 kV was used in the negative scan mode, and the cone voltage was varied between −10 to −60 V. The chemical composition of each peak was assigned by comparison of calculated and observed isotope patterns using the MassLynx 3.5 program.[14]

Synthesis of $Cs_{3.5}K\{[W_3(\mu_3\text{-}Te)(\mu_2\text{-}Te_2)_3(CN)_6]Br\}Br_{1.5}\cdot 4.5H_2O$, 1. A mixture of WTe_2 (8.00 g, 18.22 mmol), Te (0.78 g, 6.11 mmol), and Br_2 (1.90 g, 11.89 mmol) was heated in an evacuated glass ampule at 390 °C for 2 days. The resulting solid reaction product (4.00 g) was refluxed in 15 mL of H_2O with KCN (2.00 g, 30.69 mmol) for 1.5 h. The reaction solution was filtered. To the intensely colored red-brown solution was added CsCl (1.50 g, 8.91 mmol). Slow evaporation in air gave a crystalline product. Yield: 1.17 g (22%). Anal. Calcd for $C_6H_9Br_{2.5}Cs_{3.5}N_6O_{4.5}KTe_7W_3$: C, 3.02; H, 0.38; N, 3.52. Found: C, 3.03; H, 0.49; N, 3.85. IR (KBr), cm^{-1}: 2088 (ν_{CN}). ^{125}Te NMR (95 MHz, H_2O, 25 °C): δ = −36.1, −494.8, −1438.6 ppm.

Synthesis of $Cs_2K_4\{[W_3(\mu_3\text{-}Te)(\mu_2\text{-}Te_2)_3(CN)_6]_2Cl\}Cl\cdot 5H_2O$, 2. A solution of **1** (0.10 g, 0.042 mmol) in 4 mL of H_2O was added to a solution of CsCl (0.54 g, 3.21 mmol) in 2 mL of H_2O. The dark-red crystals were obtained by slow evaporation in air of the mixture. Yield: 0.070 g (86%). The complex is air stable and well soluble in water. Anal. Calcd for $C_{12}H_{10}Cs_2Cl_2N_{12}O_5K_4Te_{14}W_6$: C, 3.81; H, 0.27; N, 4.44. Found: C, 3.77; H, 0.44; N, 4.01. IR (KBr), cm^{-1}: 2091, 2061 (ν_{CN}). ES-MS (CH_3OH) (*m*/*z*; *I*, %): $[W_3Te_7(CN)_6]^{2-}$ (800.4; 75), $[W_3Te_5(CN)_6]^{2-}$ (672.8; 100), $[W_3Te_4(CN)_6]^{2-}$ (609.0; 18), $\{Cs[W_3Te_7(CN)_6]\}^-$ (1733.8; 10), $\{Cs[W_3Te_5(CN)_6]\}^-$ (1478.5; 13).

Synthesis of $(Ph_4P)_3\{[W_3(\mu_3\text{-}Te)(\mu_2\text{-}Te_2)_3(CN)_6]Br\}\cdot H_2O$, 3. A solution of Ph_4PBr (0.17 g, 0.41 mmol) in 6 mL of hot water was added to a solution of **1** (0.20 g, 0.084 mmol) in 4 mL of H_2O. The red-brown precipitate was collected by filtration, washed with water, and dried. Yield of the crude product: 0.23 g (100%). Dark-brown needlelike crystals of **3** were obtained after ether vapor diffusion into acetone solution. Anal. Calcd for $C_{78}H_{62}BrN_6OP_3Te_7W_3$: C, 34.48; H, 2.30; N, 3.09. Found: C, 34.31; H, 2.27; N, 3.39. IR (KBr), cm^{-1}: 2098, 2047 (ν_{CN}).

Synthesis of $(NH_4)_{1.5}K_3\{[Mo_3(\mu_3\text{-}Se)(\mu_2\text{-}Se_2)_3(CN)_6]I\}I_{1.5}\cdot 4.5H_2O$, 4. A mixture of $Mo_3Te_7I_4$ (1.00 g, 0.59 mmol) and KCNSe (1.67 g, 11.59 mmol) was heated in argon at 200−220 °C for 2 h. The reaction product was extracted with 10 mL of water. The solution was left in an open beaker for 2 days. The red-brown microcrystalline product was collected by filtration, washed with ethanol, and dried in air. Yield: 0.21 g (23%). Analysis (EDAX): K:Mo:Te:Se = 3.0:3.0:0.0:7.3. IR (KBr), cm^{-1}: 2107, 2063 (ν_{CN}). Raman (cm^{-1}): 560 w, 437 w, 395 w, 352 w, 305 vs, 290 sh, 265 sh, 253 vs, 218 w, 201 w, 189 w, 177 s, 154 s, 118 w, 89 sh, 63 m. ^{77}Se NMR (57 MHz, H_2O, 25 °C): δ = 615.7, 90.5, −246.8 ppm.

Synthesis of $K_3\{[W_3(\mu_3\text{-}Te)(\mu_2\text{-}SeTe)_3(CN)_6]Br\}\cdot 6H_2O$, 5. A mixture of WTe_2 (8.00 g, 18.22 mmol), Te (0.78 g, 6.11 mmol), and Br_2 (1.90 g, 11.89 mmol) was heated in an evacuated glass ampule at 390 °C for 2 days. A mixture of "$W_3Te_7Br_4$" (1.00 g, 0.57 mmol) and KCNSe (0.24 g, 1.66 mmol) was heated in argon at 190 °C for 1 h. The reaction product was extracted with 10 mL of water. The solution was left in air for 2 days. The red precipitate of Se appeared, which was removed by filtration. The dark-red crystals were obtained by evaporation of the solution. Yield: 0.072 g (7%). Analysis (EDAX): K:W:Te:Se = 3.0:3.0:4.1:3.1.

Synthesis of $K_5[W_3(\mu_3\text{-}Te)(\mu_2\text{-}Se)_3(CN)_9]$, 6. KCN (0.095 g, 1.46 mmol) was added to the solution obtained in the synthesis of **5** after removal of red selenium. The mixture was stirred for 4 h. The gray precipitate of Te appeared, which was removed by filtration.

Dark-green crystals were obtained by evaporation of the filtrate. Yield: 0.031 g (4%). Analysis (EDAX): K:W:Te:Se = 5.1:3.0:3.1:1.0. UV−vis (water; λ, nm): 351, 392, 600.

Synthesis of $K_5[W_3S_4(CN)_9]$, 7. A 1.00 g amount of $W_3S_7Br_4$ (0.91 mmol) and 2.00 g of KCNSe (13.88 mmol) were heated 3 h at 180 °C. The solidified melt was extracted with water (20 mL). The blue solution was filtered, and THF was added until an oil separated. After addition of ethanol to the oil, a dark blue precipitate of **7** was obtained. Yield: 0.20 g (20%). Analysis (EDAX): K:W:S:Se = 5.1:3.0:4.1:0.1. $[W_3S_4(CN)_9]^{5-}$ was identified by the UV−vis spectrum (water; λ/nm, $\epsilon/M^{-1}\ cm^{-1}$): 579 (370).[24]

Synthesis of $K_5[W_3Se_4(CN)_9]$, 8. A 1.00 g amount of $W_3Se_7Br_4$ (0.70 mmol) and 2.50 g of KCNSe (17.35 mmol) were heated 3 h at 180 °C. The solidified melt was extracted with water (20 mL). The green solution was filtered, and THF was added until an oil separated. After addition of ethanol to the oil, a dark green precipitate of **8** was obtained. Yield: 0.15 g (17%). Analysis (EDAX): K:W:Se = 5.0:3.1:4.1. $[W_3Se_4(CN)_9]^{5-}$ was identified by the UV−vis spectrum (water; λ/nm, $\epsilon/M^{-1}\ cm^{-1}$): 611 (860).[24] ^{77}Se NMR (57 MHz, H_2O, 25 °C): δ = 1666.1, 1133.5 ppm.

X-ray Structure Crystallography. Crystals of the complexes **1**−**6** suitable for X-ray diffraction were obtained as described above. Hemispherical data sets for **1**, **2**, and **4**−**6** were collected at T = 150 K (**5, 6**) or room temperature (**1**, **2**) on a four-circle Bruker-Nonius X8Apex CCD diffractometer using an optimized strategy

(11) (a) Fedin, V. P.; Sokolov, M. N., Virovets, A. V.; Podberezskaya, N. V.; Fedorov, V. Ye. *Polyhedron* **1992**, *11*, 2973. (b) Fedin, V. P.; Sokolov, M. N.; Gerasko, O. A.; Kolesov, B. A.; Fedorov, V. E, Mironov, Yu. V.; Yufit, D. S.; Slovokhotov, Yu. L.; Struchkov, Yu. T. *Inorg. Chim. Acta* **1990**, *175*, 217. (c) Fedin, V. P.; Sokolov, M. N.; Myakishev, K. G.; Gerasko, O. A.; Fedorov, V. Ye.; Macièek, J. *Polyhedron* **1991**, *10*, 1311.

(12) (a) Fedin, V. P.; Imoto, H.; Saito, T.; McFarlane, W.; Sykes, A. G. *Inorg. Chem*. **1995**, *34*, 5097. (b) Fedin, V. P.; Fedorov, V. Ye.; Imoto, H.; Saito, T. *Zh. Neorg. Khim*. **1997**. *42*, 1963−1973. (c) Pervukhina, N. V.; Podberezskaya, N. V.; Kalinina, I. V.; Fedin, V. P. *Zh. Strukt. Khim*. **2000**, *5*, 1027.

(13) Brixner, L. H. *J. Inorg. Nucl. Chem*. **1962**, *24*, 257.

(14) *Masslynx 3.2*; Micromass: Manchester, U.K., 1998.

Table 1. Selected Crystal and Refinement Data for **1**−**6**

param	**1**	**2**	**3**	**4**	**5**	**6**
formula	$C_6H_9Br_{2.5}Cs_{3.5}N_6O_{4.5}KTe_7W_3$	$C_{12}H_{10}Cs_2Cl_2N_{12}O_5K_4Te_{14}W_6$	$C_{78}H_{62}BrN_6OP_3Te_7W_3$	$C_6H_{15}I_{2.5}Mo_3N_{7.5}O_{4.5}K_3Se_7$	$C_6BrN_6O_6K_3Se_3Te_4W_3$	$C_9N_9K_5Se_3TeW_3$
fw	2386.00	3784.94	2716.91	1539.35	1748.16	1345.71
space group, Z	$P\bar{3}c$, 4	$Fdd2$, 16	Cc, 4	$P\bar{3}c$, 4	$P2_1$, 4	$P6_3mc$, 6
a, Å	13.1066(3)	25.626(9)	19.426(7)	12.9160(15)	8.5031(8)	18.6413(8)
a, Å	13.1066(3)	60.07(2)	19.031(6)	12.9160(15)	17.1626(13)	18.6413(8)
c, Å	23.9243(11)	15.614(5)	23.780(8)	23.080(6)	20.4991(19)	12.9868(7)
α, deg	90	90	102.885(8)	90	90	90
β, deg	90	90	90	90	93.240(2)	90
γ, deg	120	90	90	120	90	120
V, Å^3	3559.2(2)	24037(14)	8570(5)	3334.4(10)	2986.8(5)	3908.3(3)
μ(Mo Kα), mm^{-1}	21.773	19.696	6.919	11.470	20.799	19.316
d_{calc}, g cm^{-3}	4.453	4.184	2.106	3.066	3.888	3.431
$2\theta_{max}$, deg	55	55	50	50	65	59
no. of reflcns	23 018	30 466	23 748	3891	24 062	23 301
Flack		0.011(10)	0.025(11)		0.051(12)	0.08(6)
final R1, wR2 $[I > 2\sigma(I)]$[a]	0.0351, 0.0921	0.0544, 0.1173	0.0637, 0.1343	0.0423, 0.1112	0.0515, 0.1116	0.0615, 0.1212

[a] $R1 = \Sigma||F_o| - |F_c||/\Sigma|F_o|$; $wR2 = \{\Sigma[w(F_o^2 - F_c^2)^2]/\Sigma[w(F_o^2)^2]\}^{1/2}$, $w = \sigma_F^{-2}$.

based on the combination of φ- and ω-scans (graphite-monochromated Mo Kα radiation, $\lambda = 0.710\ 73$ Å, 0.5° scan range, 5−30 s/frame). A hemispherical data set for **3** was collected at room temperature on a three-cycle Bruker SMART CCD diffractometer using the standard strategy (graphite-monochromated Mo Kα radiation, $\lambda = 0.710\ 73$ Å, three ω-scans, starting $\omega = -28°$, $\phi =$ 0, 90, and 180°, detector at $2\theta = 28$, 0.3° scan range, 20 s/frame). The diffraction frames were integrated with subsequent constrained cell refinement using the SAINT package and corrected for absorption with SADABS.[15] Further experimental details are described in Table 1. Decomposition of the crystals did not occur during data collection. The structures were solved by direct methods and refined by full-matrix least-squares refinement on F^2 in anisotropic approximation for all non-hydrogen atoms (except for **3** where C, N, and O atoms were left isotropic) using the SHELXTL 5.10 software package.[16,17] In **3** the positions of all hydrogen atoms belonging to the PPh_4 groups were generated geometrically, assigned isotropic thermal parameters, and allowed to ride on their respective parent carbon atoms. In the remaining structures, hydrogen atoms of solvent water molecules were not located.

Results and Discussion

M_3Te_7 Clusters. Reactions of Mo, Te, and I_2 lead, depending on the reagents ratios, either to coordination polymer $Mo_3Te_7I_4$ or to ionic compound $[Mo_3Te_7(TeI_3)_3]I$.[18a] In the latter the external ligands TeI_3^- can be substituted by CN^- or $(RO)_2PS_2^-$ (R = Et, *i*-Pr) to give $[Mo_3Te_7(CN)_6]^{2-}$ and $[Mo_3Te_7((RO)_2PS_2)_3]I$.[12,19] The formation of $Mo_3Te_7I_4$ was also claimed to take place by heating MoI_3 and Te, based on the analytical characterization; no reactivity of that product was studied.[18b] Our initial attempts to prepare the tungsten analogues under similar conditions failed, though recently it was reported that an unidentified product obtained by heating W, Te, and I_2 in a 1:2.4:1 molar ratio did react with $(RO)_2PS_2^-$ to give $[W_3Te_7((RO)_2PS_2)_3]I$ in a 6% yield.[20] Directly substituting bromine for iodine in the syntheses does not give a product which could serve as source of W_3Te_7 in the above-mentioned reactions (the only identified crystalline material is the already known Te_7WOBr_5[21]). However, reaction of WTe_2, Te, and Br_2 in a 3:1:2 molar ratio at 390 °C does give what we presume to be "$W_3Te_7Br_4$", on the basis of its reaction with KCN solution, producing $[W_3Te_7(CN)_6]^{2-}$ in a satisfactory yield.

$$3WTe_2 + Te + 2Br_2 \rightarrow \text{“}W_3Te_7Br_4\text{”}$$

$$\text{“}W_3Te_7Br_4\text{”} + 6CN^- \rightarrow [W_3Te_7(CN)_6]^{2-} + 4Br^-$$

This result confirms that, just as in the case of W_3S_7 and W_3Se_7 cores, the W_3Te_7 core can be assembled at moderate temperatures (300−400 °C) in the halide environment.[11] The lack of single crystals prevents the structural elucidation of $Mo_3Te_7I_4$ and $W_3Te_7Br_4$, but it is reasonable to suppose that their structures are similar to their structurally characterized analogues, $Mo_3S_7Cl_4$ and $W_3S_7Br_4$.[22]

The reactivity of these telluride clusters is quite low, and only very strong nucleophiles, such as CN^-, can overcome their inertness, with $[M_3Te_7(CN)_6]^{2-}$ as products. The tungsten-containing cluster $[W_3Te_7(CN)_6]^{2-}$ was isolated in this work for the first time, as $Cs_{3.5}K\{[W_3(\mu_3\text{-}Te)(\mu_2\text{-}Te_2)_3(CN)_6]Br\}Br_{1.5}\cdot 4.5H_2O$ (**1**, Figure 1) and $Cs_2K_4\{[W_3(\mu_3\text{-}Te)(\mu_2\text{-}Te_2)_3(CN)_6]_2Cl\}Cl\cdot 5H_2O$ (**2**, Figure 1S), after addition of various amounts of CsCl to the solution of $[W_3Te_7(CN)_6]^{2-}$. Compound **1** can be converted into $(PPh_4)_3\{[W_3Te_7(CN)_6]Br\}\cdot H_2O$ (**3**, Figure 2S) by cation exchange with Ph_4PBr. All these salts show the presence of a doubly charged anion in the negative electrospray mass spectrum (ESI-MS) (cone voltage 35 V) assigned to $[W_3Te_7(CN)_6]^{2-}$. Figure 2 shows

(15) *SADABS*, version 2.11; Bruker Advanced X-ray Solutions: Madison, WI, 2004.
(16) (a) Sheldrick, G. M. *SHELX-97*; Universität Göttingen: Göttingen, Germany, 1997.
(17) Walker, N.; Stuart, D. *Acta Crystallogr., Sect. A* **1983**, *39*, 158.
(18) (a) Fedin, V. P.; Imoto, H.; Saito, T. *J. Chem. Soc., Chem. Commun.* **1995**, *34*, 5097. (b) Evstafiev, V. K. Ph.D. Thesis, Nikolayev Institute of Inorganic Chemistry, Novosibirsk, Russia, 2004.
(19) Lin, X.; Chen, H.-Y.; Chi, L.-S.; Zhuang, H.-H. *Polyhedron* **1999**, *18*, 217.
(20) Chen, H.; Lin, X.; Chi, L.; Lu, C.; Zhuang, H.; Huang, J. *Inorg. Chem. Commun.* **2000**, *3*, 331.
(21) Beck, J. *Angew. Chem., Int. Ed. Engl.* **1991**, *30*, 1128.
(22) (a) Cotton, F. A.; Kibala, P. A.; Matusz, M.; McCaleb, C. S.; Sandor, R. B. W. *Inorg. Chem.* **1989**, *28*, 2623. (b) Marcoll, J.; Rabenau, A.; Mootz, D.; Wunderlich, H. *Rev. Chim. Miner.* **1974**, *11*, 607.

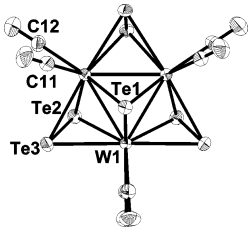

Figure 1. Molecular structure of $[W_3(\mu_3\text{-}Te)(\mu_2\text{-}Te_2)_3(CN)_6]^{2-}$ in **1** with the atom-labeling scheme and 50%-probability thermal ellipsoids.

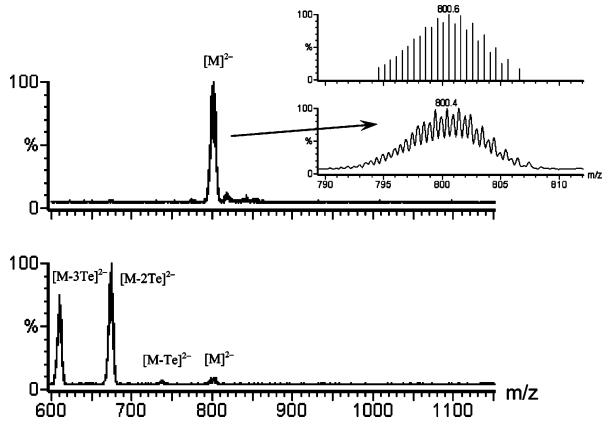

Figure 2. ESI-MS spectra of the dianion $[W_3Te_7(CN)_6]^{2-}$ in the negative scan mode at 35 (top) and 55 V (bottom). The inset shows the observed together with the simulated molecular peak using the natural isotope abundance distribution.

the mass spectrum recorded at 35 and 55 V. Increasing the cone voltage up 50 V results in consecutive losses of three tellurium atoms to give a species formulated as $[W_3Te_4(CN)_6]^{2-}$. Further increasing the cone voltage to 55 V result in cyanide dissociation to afford the monoanionic species $[W_3Te_4(CN)_5]^-$.

$$[W_3Te_7(CN)_6]^{2-} \xrightarrow[-Te]{} [W_3Te_6(CN)_6]^{2-} \xrightarrow[-Te]{} [W_3Te_5(CN)_6]^{2-} \xrightarrow[-Te]{} [W_3Te_4(CN)_6]^{2-} \xrightarrow[-CN]{} [W_3Te_4(CN)_5]^-$$

In the case of **2**, low-intensity peaks due to ionic associates $\{Cs[W_3Te_7(CN)_6]\}^-$ and $\{Cs[W_3Te_5(CN)_6]\}^-$ were also observed. A similar fragmentation pattern of consecutive chalcogen loss has been reported for related sulfur- and selenium-containing complexes $Mo_3Q_7^{4+}$ (Q = S, Se) using FAB or L-SIMS mass spectrometry, where stepwise abstraction of three chalcogen and ligand dissociation of one bidentate outer ligand are observed.[23]

The coordinated CN^- ligand is observed in the IR spectrum as intense bands at 2088 cm^{-1} (**1**) and 2091 and 2061 cm^{-1} (**2**), which are comparable with 2100 cm^{-1} for $[Mo_3Te_7(CN)_6]^{2-}$ in the double salt $Cs_{2.5}K_2\{[Mo_3Te_7(CN)_6]I\}\text{-}I_{1.5}\cdot 3H_2O$.[12]

Reactions with KNCSe Melt. Our original idea was to use low-melting KNCSe to effectuate ligand substitution in polymeric $M_3Te_7I_4$ and their S and Se analogues, by heating

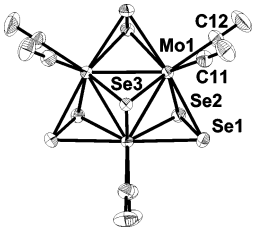

Figure 3. Molecular structure of $[Mo_3(\mu_3\text{-}Se)(\mu_2\text{-}Se_2)_3(CN)_6]^{2-}$ in **4** with partial atom-labeling scheme and 50%-probability thermal ellipsoids.

Table 2. Reactions of $M_3Q_7X_4$ with Molten KNCSe

reagent	final product	obsd intermediates
$Mo_3Te_7I_4$	$[Mo_3Se_7(CN)_6]^{2-}$	$[Mo_3Te_4Se_3(CN)_6]^{2-}$
$W_3Te_7Br_4$	$[W_3Se_7(CN)_6]^{2-}$ [c]	$[W_3Te_4Se_3(CN)_6]^{2-}$,[a] $[W_3Te_3Se_4(CN)_6]^{2-}$, $[W_3Se_5Te_2(CN)_6]^{2-}$, $[W_3Se_6Te(CN)_6]^{2-}$
$Mo_3Se_7Br_4$	$[Mo_3Se_7(CN)_6]^{2-}$	
$W_3Se_7Br_4$	$[W_3Se_4(CN)_9]^{5-}$	
$Mo_3S_7Br_4$	$[Mo_3Se_7(CN)_6]^{2-}$	$[Mo_3SSe_6(CN)_6]^{2-}$, $[Mo_3S_4Se_3(CN)_6]^{2-}$
$W_3S_7Br_4$	$[W_3S_4(CN)_9]^{5-}$ [b]	

[a] Isolated. [b] Shorter reaction times. [c] Not isolated pure.

the solids in the KNCSe melt (200 °C). In no case $NCSe^-$ complexes could be isolated; instead, chalcogen substitution in the cluster core took place, with the formation of different products depending on the starting cluster chalcogenide (Table 2). In the case of $Mo_3Te_7I_4$ we obtained, after extraction with water, a dark red solution, from which red-brown crystals of $(NH_4)_{1.5}K_3\{[Mo_3(\mu_3\text{-}Se)(\mu_2\text{-}Se_2)_3(CN)_6]I\}\text{-}I_{1.5}\cdot 4.5H_2O$ (**4**, Figure 3) were isolated. The NH_4^+ obviously comes from the partial decomposition of the $NCSe^-$. Thus, complete exchange of the chalcogen in the cluster core takes place under these reaction conditions.

$$Mo_3Te_7I_4 + 7KCNSe \rightarrow K_2[Mo_3Se_7(CN)_6] + 7Te + 4KI + KCN$$

It must be stressed that the complex $[Mo_3Se_7(CN)_6]^{2-}$ is not available by direct reaction of polymeric $Mo_3Se_7Br_4$ with KCN (in contrast to the telluride), which instead gives $[Mo_3Se_4(CN)_9]^{5-}$ after Se abstraction from the three Se_2 bridging ligands.[24]

$$Mo_3Se_7Br_4 + 12KCN \rightarrow K_5[Mo_3Se_4(CN)_9] + 3KCNSe + 4KBr$$

$[Mo_3Se_4(CN)_9]^{5-}$ is quantitatively obtained in reaction of $[Mo_3Se_7(CN)_6]^{2-}$ with free CN^- in aqueous solution:

$$[Mo_3Se_7(CN)_6]^{2-} + 6CN^- \rightarrow [Mo_3Se_4(CN)_9]^{5-} + 3CNSe^-$$

Molten KNCSe is in equilibrium with KCN and Se. To explain why the CN^- present in the KCNSe melt failed to convert $[Mo_3Se_7(CN)_6]^{2-}$ into $[Mo_3Se_4(CN)_9]^{5-}$ the following equilibrium must be considered:

$$Mo_3Se_7^{4+} + 3CN^- = Mo_3Se_4^{4+} + 3NCSe^-$$

The equilibrium is shifted to the right in the reaction between

(23) Hegetschweiler, K.; Caravatti, P.; Fedin, V. P.; Sokolov, M. N. *Helv. Chim. Acta* **1992**, *75*, 1659.

(24) Fedin, V. P.; Lamprecht, G. J.; Kohzuma, T.; Clegg, W.; Elsegood, M. R. J.; Sykes, A. G. *J. Chem. Soc., Dalton Trans.* **1997**, 1747.

Scheme 1

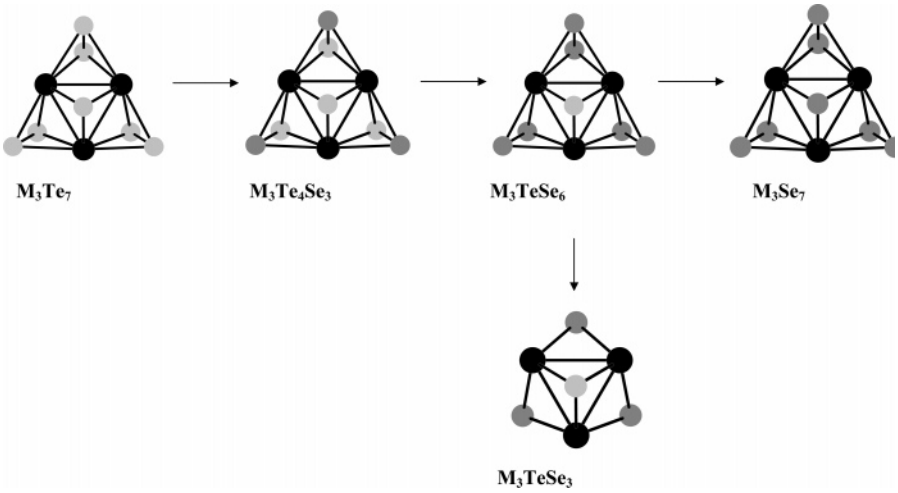

$Mo_3Se_7Br_4$ with aqueous solution of KCN, in which an excess of KCN was used, and to the left in the melt, where KNCSe is in excess. The compatibility of Se_2^{2-} (as reaction product) with CN^- (as reagent) is corroborated by the preparation of Se_2-bridged chain of $\{Re_6Se_8(CN)_4\}$ units in $K_6[Re_6Se_{10}(CN)_4]$ in the reaction of $ReSe_2$ with KCN at 650 °C.[25] That the real reaction takes place stepwise can be seen from ESI-MS of the crude products, which shows not only dominant peaks of $[Mo_3Se_7(CN)_6]^{2-}$ but also another (minor) peak due to $[Mo_3Te_4Se_3(CN)_6]^{2-}$. If we assume that the Te/Se exchange occurs as regioselective as the S/Se one,[26] the Se atoms must occupy the equatorial positions of the $M_3(\mu_3\text{-}Q)(\mu\text{-}Q_{ax.}\text{-}Q_{eq.})_3^{4+}$ core. The reaction of $Mo_3Se_7Br_4$ with molten KCNSe is a more direct and clean way to $[Mo_3Se_7(CN)_6]^{2-}$. Thus, under these conditions, 1.00 g of $Mo_3Se_7Br_4$ (0.86 mmol) and 1.50 g of KCNSe (10.41 mmol) give 0.34 g of the red-brown microcrystalline product ($[Mo_3Se_7(CN)_6]^{2-}$ was detected by ESI-MS). The $Mo_3S_7^{4+}$ clusters in solution undergo regiospecific Se for S substitution into the equatorial positions, leading to the $Mo_3S_4Se_3^{4+}$ clusters, as can be illustrated by the synthesis of $[Mo_3S_4Se_3(Et_2NCS_2)_3]^+$ from $[Mo_3S_7(Et_2NCS_2)_3]^+$ and KNCSe in CH_3CN solution, already at room temperature.[26] In the KCNSe melt at 200−220 °C the chalcogen exchange progresses further, with $[Mo_3S_4Se_3(CN)_6]^{2-}$ and $[Mo_3SSe_6(CN)_6]^{2-}$ as intermediates (detected by ESI-MS) and $[Mo_3Se_7(CN)_6]^{2-}$ as the final product. From the stoichiometry we may assume that the intermediate $[Mo_3SSe_6(CN)_6]^{2-}$ still retains sulfur in the capping (μ_3) position. Thus, the relative lability of chalcogen atoms in the three different positions of $M_3(\mu_3\text{-}Q)(\mu\text{-}Q_{ax.}\text{-}Q_{eq.})_3^{4+}$ cores is $Q_{eq} > Q_{ax} > \mu_3\text{-}Q$.

The only other example of the replacement of bridging Te by Se is the transformation of tetrahedral cluster $[Re_4Te_4(TeCl_2)_4Cl_8]$ into octahedral $[Re_6Se_8(CN)_6]^{4-}$ by KNCSe in superheated CH_3CN at 200 °C.[27]

Reaction of "$W_3Te_7Br_4$" with KNCSe in melt allowed the isolation of a mixed Se/Te cluster, $K_3\{[W_3(\mu_3\text{-}Te)(\mu_2\text{-}SeTe)_3(CN)_6]Br\}\cdot 6H_2O$ (**5**, Figure 4). The Se atoms selectively enter into the equatorial positions of the μ_2-Q_2 ligands, thus giving access to previously practically unknown complexes of $SeTe^{2-}$, which can be regarded as a new inorganic ligand. The only other example of a SeTe complex is found in $[Fe_2(\mu\text{-}SeTe)(CO)_6]$ which can be prepared "in pure form and in good yields", but the characterization is based solely upon chromactographic behavior, reactivity, and IR in the CO region.[28] Another well-defined mixed Se/Te ligand, open-chained $[Se-Te-Te-Se]^{2-}$, is obtained by selective substitution of the central Se atoms in $[Hg(Se_4)_2]^{2-}$ (those not bound with Hg) with Et_3PTe. This reaction is also regioselective.[29]

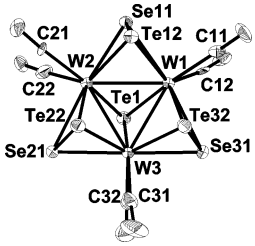

Figure 4. Molecular structure of $[W_3(\mu_3\text{-}Te)(\mu_2\text{-}SeTe)_3(CN)_6]^{2-}$ in **5** with partial atom-labeling scheme and 50%-probability thermal ellipsoids.

In fact the reaction proceeds stepwise, and the monitoring by ESI-MS shows the sequential formation of $[W_3Se_3Te_4(CN)_6]^{2-}$ (m/z = 728), $[W_3Se_4Te_3(CN)_6]^{2-}$ (m/z = 704), $[W_3Se_5Te_2(CN)_6]^{2-}$ (m/z = 680), $[W_3Se_6Te(CN)_6]^{2-}$ (m/z = 656), and $[W_3Se_7(CN)_6]^{2-}$ (m/z = 632). The proposed sequence is shown in Scheme 1. The latter complex is not particularly stable under the reaction conditions, and the reaction between $W_3Se_7Br_4$ and KNCSe always yields $[W_3Se_4(CN)_9]^{5-}$.

The tungsten clusters show a lesser stability of the $W_3Q_7^{4+}$ core, which more or less easily loses three chalcogen atoms of μ_2-Q_2 ligands, giving more stable $W_3Q_4^{4+}$ clusters. For example, $[W_3S_7Br_6]^{2-}$ gives $[W_3S_4(NCS)_9]^{5-}$ already by heating with KNCS in acetonitrile solution.[11b] It is no surprise, then, that the tungsten clusters $W_3Se_7Br_4$ and W_3S_7-

(25) Mironov, Y. V.; Fedorov, V. E.; McLauchlan, C. C.; Ibers, J. A. *Inorg. Chem.* **2000**, *39*, 1809.
(26) Fedin, V. P.; Sokolov, M. N.; Virovets A. V.; Podberezskaya N. V.; Fedorov, V. Ye. *Polyhedron* **1992**, *11*, 2395.
(27) Eanes, M. E.; Ibers, J. A. *Inorg. Chem.* **2002**, *41*, 6170.
(28) Mathur, P.; Chakrabarty, D.; Munkir Hossain, Md. *J. Organomet. Chem.* **1991**, *401*, 167.

Table 3. Selected Bond Lengths (Å) for **1**−**6**

param	1	2	3	4	5	6
M−M	2.87	2.86−2.89	2.88	2.78	2.82−2.83	2.82−2.86
M−μ_3-Q	2.71	2.71−2.73	2.70−2.71	2.54	2.71	2.67−2.69
M−Q_{eq}	2.81−2.82	2.80−2.85	2.80−2.82	2.61-2.62	2.64−2.65	
M−Q_{ax}	2.74−2.76	2.74−2.77	2.74−2.76	2.56	2.72−2.74	2.43−2.47
M−C_{trans}[a]	2.16	2.06−2.18	2.11−2.21	2.17	2.13−2.19	2.05−2.37
M−C_{cis}[b]	2.12	1.59−2.25	2.12−2.20	2.15	2.10−2.16	1.96−2.30
Q_{eq}−Q_{ax}	2.69	2.68−2.70	2.68	2.35	2.50−2.52	

[a] M−C_{trans} distance trans to M−μ_3-Q bond. [b] M−C_{cis} distance cis to M−μ_3-Q bond.

Br_4 give only the chalcogen-poor incomplete cuboidal clusters under similar conditions: $[W_3Se_4(CN)_9]^{5-}$ in the first case and $[W_3S_4(CN)_9]^{5-}$ in the second case. Pure $K_5[W_3Q_4(CN)_9]$ (Q = S, **7**; Q = Se, **8**) can be isolated by adding a large volume of THF to the aqueous extracts after melting and cooling. The ESI-MS spectra of **7** and **8** show the peaks of $[W_3Q_4(CN)_6]^{2-}$ (from the loss of three CN^- by unobservable parent $[W_3Q_4(CN)_9]^{5-}$) and of $[W_3Q_3(CN)_6]^{2-}$. The excess of negative charge carried by the 5− anions $[W_3Q_4(CN)_9]^{5-}$ prevents its appearance in the gas phase, and only the more stable ligand dissociation products, i.e., dianions, are observed.

The electronic spectra are characteristic and correspond to that reported for the $[W_3Q_4(CN)_9]^{5-}$ species prepared from $W_3Q_7Br_4$ and aqueous solution of KCN.[24] The ^{77}Se NMR spectrum of $[W_3(\mu_3\text{-Se})(\mu_2\text{-Se})_3(CN)_9]^{5-}$ shows, as expected, two signals at 1666.1 and 1133.5 ppm. In $[W_4(\mu_3\text{-Se})_4(CN)_{12}]^{6-}$ the signal from μ_3-Se is observed at 1496 ppm.[30] KNCS in melt under similar conditions converts $W_3S_7Br_4$ and $W_3Se_7Br_4$ into $[W_3S_4(NCS)_9]^{5-}$ (via intermediate species $[W_3S_xSe_{4-x}(NCS)_9]$).[5−31] The NCS^- ion is more stable than $NCSe^-$, and no formation of the competing CN^- takes place under the experimental conditions.

In the reactions studied in this work, the M^{IV}_3 triangle unit is preserved. It is thus stable in the presence of QCN^-/CN^- at least up to 220 °C. Raising the temperature up to 450 °C does lead to reduction and transformation into cuboidal clusters with tetrahedral $M^{III}_2M^{IV}_2$ cores.[30] Even more drastic conditions (650 °C) would possibly favor the formation of even more reduced $[Mo_6Q_8(CN)_6]^{6-/7-}$ clusters.[32]

$W_3(\mu_3\text{-Te})(\mu\text{-Se})_3^{4+}$ Cluster. By adding KCN to the extract from the reaction of $W_3Te_7Br_4$ with KNCSe, we obtained a $W_3(\mu_3\text{-Te})(\mu\text{-Se})_3^{4+}$ complex, $K_5[W_3(\mu_3\text{-Te})(\mu_2\text{-Se})_3(CN)_9]$ (**6**, Figure 5). The attack takes place either at Te in $[W_3Se_3Te_4(CN)_6]^{2-}$ ($TeCN^-$ initially formed is unstable in aqueous solution and decomposes into CN^- and Te; the precipitation of the latter was observed) or at Se in $[W_3Se_6Te(CN)_6]^{2-}$. Also, it is not possible to exclude the initial attack on Se with subsequent Se/Te interchange with $SeCN^-$. The $M_3Q_4^{4+}$ cores are susceptible to chalcogen exchange show the unexpected preparation of a $W_3(\mu_3\text{-S})(\mu\text{-Te})_3^{4+}$ cluster, $[Mo_3STe_3(dtp)_3(PAB)(PBu_3)]$ (dtp = $(i\text{-PrO})_2PS_2$, PAB = *para*-aminobenzoate), from $[Mo_3Te_7(dtp)_3]I$. The sulfur atom comes from the dithiophosphate ligand.[34]

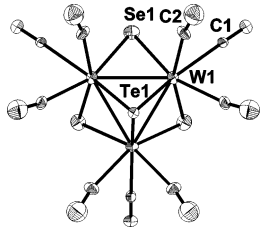

Figure 5. Molecular structure of $[W_3(\mu_3\text{-Te})(\mu_2\text{-Se})_3(CN)_9]^{5-}$ in **6** with partial atom-labeling scheme and 50%-probability thermal ellipsoids.

Crystal Structures. Crystal structures were determined for $Cs_{3.5}K\{[W_3(\mu_3\text{-Te})(\mu_2\text{-Te}_2)_3(CN)_6]Br\}Br_{1.5}\cdot 4.5H_2O$ (**1**), $Cs_2K_4\{[W_3(\mu_3\text{-Te})(\mu_2\text{-Te}_2)_3(CN)_6]_2Cl\}Cl\cdot 5H_2O$ (**2**), $(Ph_4P)_3\{[W_3Te_7(CN)_6]Br\}\cdot H_2O$ (**3**), $(NH_4)_{1.5}K_3\{[Mo_3Se_7(CN)_6]I\}I_{1.5}\cdot 4.5H_2O$ (**4**), $K_3\{[W_3(\mu_3\text{-Te})(\mu_2\text{-SeTe})_3(CN)_6]Br\}\cdot 6H_2O$ (**5**), and $K_5[W_3(\mu_3\text{-Te})(\mu_2\text{-Se})_3(CN)_9]$ (**6**). The observed geometrical parameters of $[M_3Q_7(CN)_6]^{2-}$ are summarized in Table 3. In all cases these anions are heavily involved in secondary (specific nonbonding) interactions with the halide mainly through $3Q_{ax}\cdots X^-$ contacts, which are sometimes supported by $Q_{eq}\cdots X^-$ or by $Q_{eq}\cdots Q_{eq}$. interactions. As in the case of $M_3S_7^{4+}$ and $M_3Se_7^{4+}$ clusters, these contacts are much shorter then the sum of van der Waals radii of corresponding elements.[35,36] Thus {anion + anion} aggregates $\{[W_3Te_7(CN)_6]Cl\}^{3-}$, $\{[W_3Te_7(CN)_6]Br\}^{3-}$, $\{[Mo_3Se_7(CN)_6]I\}^{3-}$, and $\{[W_3Te_4Se_3(CN)_6]Br\}^{3-}$ form via three symmetrically equivalent $Te_{ax}\cdots Br^-$ contacts (3.420(2) Å) for **1**, three $Te_{ax}\cdots Cl^-$ contacts (3.152(9)−3.276(9) Å) for **2,** three $Te_{ax}\cdots Br^-$ contacts (3.198(4)−3.304(3) Å) for **3**, three symmetrically equivalent $Se_{ax}\cdots I^-$ contacts (3.446(1) Å) for **4**, and three nonequivalent $Te_{ax}\cdots Br^-$ contacts for **5** (3.067(2)−3.236(3) Å, Figure 6). It should be noted that the length of $Q_{ax}\cdots X$ contacts does not exclusively depend on the nature of Q and X. Indeed, the van der Waals radii of X vary from 1.80 Å for Cl^- to 2.15 Å for I^- (in the Pauling system[35]). It means that if we assume the "usual", nonspecific nature of $Q\cdots X$ interaction the Te···I distance should be at

(29) Bollinger, J. C.; Ibers, J. A. *Inorg. Chem.* **1995**, *34*, 1859.
(30) Fedin, V. P.; Kalinina, I. V.; Samsonenko, D. G.; Mironov, Y. V.; Sokolov, M. N.; Tkachev, S. V.; Virovets, A. V.; Podberezskaya, N. V.; Elsegood, M. R. J.; Clegg, W.; Sykes, A. G. *Inorg. Chem.* **1999**, *38*, 1956.
(31) Fedorov, V. E.; Mûller, A.; Fedin, V. P.; Sokolov, M. N. *Zh. Neorg. Khim.* **1994**, *39*, 1663.
(32) (a) Mironov, Y. V.; Virovets, A. V.; Naumov, N. G.; Ikorski, V. N.; Fedorov, V. E. *Chem.*—Eur. J. **2000**, *6*, 1361. (b) Magliocchi, C.; Xie, X.; Hughbanks, T. *Inorg. Chem.* **2000**, *39*, 5000.
(33) Saysell, D.; Fedin, V. P.; Lamprecht, G. J.; Sokolov, M. N.; Sykes, A. G. *Inorg. Chem.* **1997**, *36*, 2982.
(34) Lin, X.; Chen, H.-Y.; Chi, L.-S.; Lu, C.-Zh.; Zhuang, H.-H. *Polyhedron* **2000**, *19*, 925.
(35) Batsanov, S. S. *Russ. J. Inorg. Chem.* **1991**, *36*, 1694.
(36) Virovets, A. V.; Podberezskaya, N. V. *Zh. Struct. Khim.* **1993**, *34*, 150.

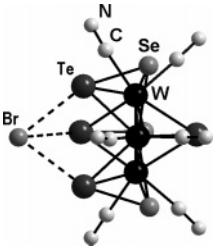

Figure 6. Structure of the adduct $\{[W_3Te_4Se_3(CN)_6]Br\}^{3-}$ in **5**.

Table 4. Interatomic Distances $d(Q_{ax}\cdots X)$ and Covalence Indices f_{cov} for the $Q_{Ax}\cdots X$ Interactions[a] in the $\{[M_3Q_7(CN)_6]X\}^{3-}$ Adducts

formula	$d(Q_{ax}\cdots X)$, Å	f_{cov}	ref
1	3.42	0.41	this work
2	3.15−3.28	0.49	this work
3	3.20−3.30	0.55	this work
4	3.45−3.49	0.42	this work
5	3.07−3.24	0.63	this work
$Cs_{4.5}[Mo_3Te_7(CN)_6]I_{2.5}\cdot 3H_2O$	3.58	0.45	12a

[a] $f_{cov} = [R_{vdW}(Q) + R_{vdW}(X) - d(Q_{ax}-X)][R_{vdW}(Q) + R_{vdW}(X) - R_{cov}(Q) - R_{cov}(X)]^{-1}$, where R_{vdW} and R_{cov} are the van der Waals radii and covalent radii of the corresponding atoms.

least by 0.35 Å longer than $Te_{ax}\cdots Cl$ one. In reality, this difference is only about 0.25 Å (3.45 Å in **4** vs. 3.20 Å in **2**). In the same time, average the $Te_{ax}\cdots Br$ distance in **5** is only 3.15 Å, even shorter then $Te_{ax}\cdots Cl$ in **2**! It confirms the specific nature of 3 $Te_{ax}\cdots X$ interactions,[32,33,36] which become increasingly important in the order Cl < Br < I.

To analyze such contacts, a semiempirical parameter, the covalence factor (f_{cov}), was found to be useful (Table 4). $f_{cov} = 0$ corresponds to no bonding, and $f_{cov} = 1$, to normal covalent bonding.[35−37] The contacts of about 3.1−3.6 Å observed for $\{[M_3Q_7(CN)_6]X\}^{3-}$ represent a significant degree of bonding ($f_{cov} = 0.4-0.6$).

The specific interactions with Se and Te atoms of the $M_3Q_7^{4+}$ cluster core play the key role in the formation of crystal packings of **1**−**5**. The most interesting case here is **2,** where the relatively small cluster anions (the longest dimension in $[W_3Te_7(CN)_6]^{2-}$ is in the $N\cdots Te_{eq}$ direction (8.1 Å), small Cs^+, K^+, and Cl^-, and water molecules generate fantastically complicated packing with quite rare *Fdd*2 space symmetry, 16 formula units/unit cell, and one of the cell parameters, *b*, about 60 Å. The reason is the presence of various types of specific interactions. In this structure there are two crystallographically independent cluster anions with different structural roles. One of them forms a $\{[W_3Te_7(CN)_6]Cl\}^{3-}$ aggregate with 3 $Te_{ax}\cdots Cl$ contacts (see above). Then, one of its CN groups make three short $Te_{ax}\cdots N$ contacts of 2.87(2), 2.95(2), and 3.30(2) Å with another cluster anion resulting in zigzag chains. There are also two short contacts $Te_{eq}\cdots N$ (2.97(3), 3.38(3) Å) between two neighboring clusters, which also participate in the chain formation (Figure 7). Therefore, all atoms Te_{ax} are involved in specific interactions with chlorine anions and nitrogen atoms of the CN ligands. In addition, there is a quite

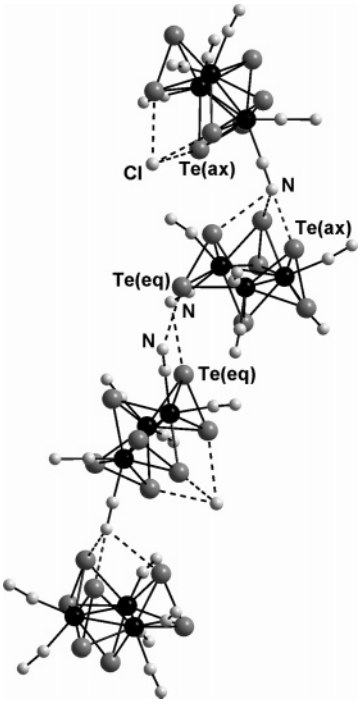

Figure 7. Fragment of the crystal structure of **2**. Key: black circles, W; medium gray, Te; light gray, Cl, C, N. Other atoms are omitted for clarity. The Te···Cl and Te···N contacts are shown as dashed lines.

long $Te_{eq}\cdots Cl$ contact of 3.886(8) Å corresponding to an additional, weaker interaction. These contacts together with alkaline metal cations combine the chains into a 3D framework.

In the crystal structure of **5** there are linear chains running along the *x* axis. The bromine anions form three contacts with 3 Te_{ax} and one additional short contact of 3.205(2) Å with Se_{eq} of the neighboring $\{[W_3Te_4Se_3(CN)_6]Br\}^{3-}$ aggregate.

Another interesting packing motif can be seen in **1** and **4**, where the $\{[W_3Te_7(CN)_6]Br\}^{3-}$ and $\{[Mo_3Se_7(CN)_6]I\}^{3-}$ aggregates are bound into corrugated layers running parallel to *ab* plane via linear, symmetrical $Te_{eq}\cdots Br^-\cdots Te_{eq}$ and $Se_{eq}\cdots I^-\cdots Se_{eq}$ contacts of 3.3405(7) and 3.489(1) Å, respectively, with the participation of extra halogen anions (Figure 8). The compounds **1** and **4** are isostructural with $K_{4.5}\{[Mo_3(\mu_3\text{-}Te)(\mu_2\text{-}Te_2)_3(CN)_6]I\}I_{1.5}\cdot 3H_2O$, $Cs_{2.29}K_{2.21}\{[Mo_3(\mu_3\text{-}Te)(\mu_2\text{-}Te_2)_3(CN)_6]I\}I_{1.5}\cdot 3H_2O$, and $Cs_{4.5}\{[Mo_3(\mu_3\text{-}Te)(\mu_2\text{-}Te_2)_3(CN)_6]I\}I_{1.5}\cdot 3H_2O$.[12]

The geometrical parameters of the cluster cores in **1**−**6** are strongly dependent on the bridging chalcogen (Table 3). While changes from Mo to W and in the nonbridging ligands hardly influence the M−M bond lengths (for example, the Mo−Mo distances are in $Cs_{4.5}\{[Mo_3(\mu_3\text{-}Te)(\mu_2\text{-}Te_2)_3(CN)_6]I\}I_{1.5}\cdot 3H_2O$ 2.891(2) Å,[12] in $[Mo_3Te_7((EtO)_2PS_2)_3]I$ 2.89−2.90 Å,[19] in $[W_3Te_7((EtO)_2PS_2)_3]I$ 2.84−2.85 Å,[20] in **1** and **2** 2.86−2.89 Å, and in **3** 2.88 Å), the change from Te to Se decreases the M−M distances by about 0.1 Å (the Mo−Mo distance in **4** is 2.78 Å). As can be expected, the effect of the mixed ligand $TeSe^{2-}$ is intermediate (the W−W distances are 2.82−2.83 Å in **5**). The order of M−Te bond lengths is $M-\mu_3\text{-}Te < M-Te_{ax} < M-Te_{eq}$, spanning the range of more

(37) Mayor-Lopez, M.; Weber, M.; Hegetschweiler; K.; Meienberger, M. D.; Jobo, F.; Leoni, S.; Nesper, R.; Reiss, G. J.; Frank W.; Kolesov, B.; Fedin, V.; Fedorov, V. *Inorg. Chem.* **1998**, *37*, 2633.

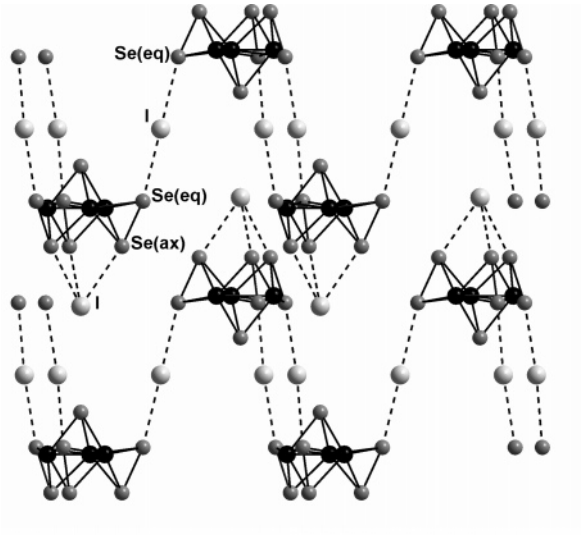

Figure 8. Fragment of crystal structure of **4**, view along the *b* axis. Key: black circles, Mo; medium gray, Se; light gray, I. Other atoms are omitted for clarity. The Se···I contacts are shown as dashed lines.

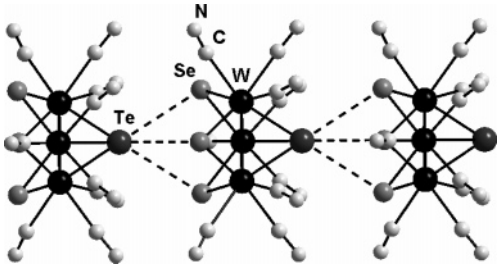

Figure 9. Fragment of crystal structure of **6**. The Se_{ax}···Te contacts of 3.603(7) Å are shown as dashed lines.

than 0.1 Å, and the absolute values are close to those for other M_3Te_7 clusters.[18−20] The same sequence was found for the Mo−Se bonds in **4**.[38] In the chalcogen-mixed cluster **5**, the W−Se_{eq} distances are close to those found in the $W_3Se_7^{4+}$ clusters, such as $[W_3Se_7(Et_2NCS_2)_3]^+$ and $[W_3Se_7((EtO)_2PS_2)_3]^+$,[39] and the W−Te distances are roughly inside the range observed in **1**−**3** and in $[W_3Te_7((EtO)_2PS_2)_3]I$.[20] This shows that the M−M interactions are more flexible than the M−Q ones and adapt themselves to the sterical constraints imposed on the molecular architecture by the chalcogen size. There are two other types of W/Te clusters, where all the Te atoms are of μ_3 type: the cuboidal clusters $[W_4Te_4(CN)_{12}]^{6-}$ (W−Te, 2.69 Å; W−W, 2.86 Å)[30] and the octahedral clusters $[W_6Te_8L_6]$ (L = PEt_3, py, piperidine) (W−Te, 2.74−2.76 Å; W−W, 2.73−2.77 Å).[40] The Te−Te bonds are by 0.10−0.15 Å shorter than in elemental tellurium (2.835 Å). This difference is somewhat intriguing, since in the $M_3S_7^{4+}$ and $M_3Se_7^{4+}$ cores the S−S and Se−Se bonds have the same lengths as in elemental chalcogens (2.05−2.08 Å in S_8, 2.30-(1) Å in gray Se).[41] On the other hand, in $[Me_4N]_2[Te_2]$ and $[Na(CH_3OH)_3]_2[Te_2]$, the Te−Te bond lengths are 2.737(1) and 2.744(1) Å, respectively.[42] In both complexes the $[Te_2]^{2-}$ dumbbells are well separated and do not interact. The Te−Se bond distance in **5**, 2.50−2.52 Å, has the same value as in the V-shaped anion $[SeTeSe]^{2-}$, present in [K(2,2,2-crypt)]$_2TeSe_2$·en and in $[Mn(en)_3]TeSe_2$ (2.50 Å) (formally a single bond), and is expectedly longer than 2.46−2.47 Å in [K(2,2,2-crypt)]$_2TeSe_3$·en (formal bond order 4/3 in the pyramidal $TeSe_3^{2-}$).[43]

The structure of $[W_3TeSe_3(CN)_9]^{5-}$ in **6** is shown in Figure 5. The W−W distances are 2.82−2.86 Å, W−Se are 2.43−2.47 Å, and W−Te are 2.67−2.69 Å. Closely related $[W_3Se_4(CN)_9]^{5-}$, which differs only by the presence of Se in the μ_3 position, is found in the double salt $Cs_5[W_3Se_4(CN)_9]$·CsCl·$4H_2O$ and has the following (mean) interatomic distances: W−W, 2.829 Å; W−Se, 2.449 Å; W−(μ_3-Se), 2.497 Å.[24] It is immediately apparent that this change from $W_3Se_4^{4+}$ to $W_3TeSe_3^{4+}$ does not affect (geometrically) the rest of the cluster. The W−μ_3-Te bond in **6** is somewhat shorter than in the heptachalcogenide clusters in **1**−**3** and **5**. In the crystal the anions $[W_3TeSe_3(CN)_9]^{5-}$ are oriented in the same direction ("face-to-tail") and stack to form the columns running along the *c* axis. Within the columns, three short Te···Se contacts (3.603(7) Å) form between neighbors (Figure 9). The intercolumnar space is filled with potassium cations which interact with nitrogen atoms of the cyanide ligands (2.6−3.0 Å). Such a packing motif is new for $M_3Q_4^{4+}$ clusters but can be seen in some $M_3Q_7^{4+}$ ones, e.g. in $(NH_4)_2[Mo_3S_7(S_2)_3]$ (S_{ax}···μ_3-S are of 3.02 Å).[44] This way of packing is radically different from what is observed in the structures of $Cs_5[W_3Se_4(CN)_9]$·CsCl·$4H_2O$,[24] $[W_3Se_4(H_2O)_9](p\text{-}CH_3C_6H_4SO_3)_4$·$12H_2O$,[45] and $(Me_3NH)_5[W_3Se_4(NCS)_9]$,[11] where the cluster anions are weakly dimerized through "face-to-face" μ_2-Se···μ_2-Se interactions.

The importance of specific interactions between heavier nonmetals is increasingly being recognized. In addition to halogen−halogen, chalcogen−chalcogen, and pnictogen−pnictogen interactions[46−48] (and, of course, to the already classical H-bonding and $\pi-\pi$ stacking), the chalcogen−halogen contacts must be added to the list of noncovalent

(38) Sokolov, M. N.; Gushchin, A. L.; Naumov, D. Yu.; Gerasko, O. A.; Fedin, V. P. *Inorg. Chem.* **2005**, *44*, 2431.
(39) (a) Fedin, V. P.; Sokolov, M. N.; Gerasko, O. A.; Virovets, A. V.; Podberezskaya, N. V.; Fedorov, V. Ye. *Polyhedron* **1992**, *11*, 3159. (b) Fedin, V. P.; Sokolov, M. N.; Gerasko, O. A.; Virovets, A. V.; Podberezskaya, N. V.; Fedorov, V. Ye. *Inorg. Chim. Acta* **1991**, *187*, 81.
(40) Xie, X.; McCarley, R. E. *Inorg. Chem.* **1997**, *36*, 4665.
(41) (a) Templeton, L. K.; Templeton, D. H.; Zalkin, A. *Inorg. Chem.* **1976**, *15*, 1999−2001. (b) Avilov, A. S.; Imanov, R. M. *Kristallografiya* **1969**, *14*, 230.
(42) (a) Batchelor, R. J.; Einstein, F. W. B.; Gay, I. D.; Jones, C. H. W.; Sharma, R. D. *Inorg. Chem.* **1993**, *32*, 4378. (b) Thiele, K.-H.;. Steinicke, A.; Dümichen, U.; Neumüller, B. *Z. Anorg. Allg. Chem.* **1996**, *622*, 231.
(43) (a) Bjorgvisson, M.; Sawyer, J. F.; Schrobilgen, G. J. *Inorg. Chem.* **1991**, *30*, 4238. (b) Wendland, F.; Nather, C.; Bensch, W. *Z. Naturforsch., B: Chem. Sci.* **2000**, *55*, 871. (c) Bjorgvisson, M.; Sawyer, J. F.; Schrobilgen, G. J. *Inorg. Chem.* **1991**, *30*, 4238.
(44) Müller, A.; Pohl, S.; Dartmann, M.; Cohen, J. P.; Bennett, M. J.; Kirschner, R. M. *Z. Naturforsch.* **1979**, *B34*, 434.
(45) Hernandez-Molina, R.; Elsegood, M. R. J.; Clegg, W.; Sykes, A. G. *J. Chem. Soc., Dalton Trans.* **2001**, 2173.
(46) Pedireddi, V. R.; Reddy, D. S.; Goud, B. S.; Craig, D. C.; Rae, A. D.; Desiraju, G. R. *J. Chem. Soc., Perkin Trans. 2* **1994**, 2353.
(47) Gleiter, R.; Werz, D.; Rausch, B. *Chem.*−Eur. J. **2003**, *9*, 2677.
(48) *Unkoventionelle Wechselwirkungen in der Chemie Metallischer Elemente*; Forschungsbericht DFG; Krebs, B., Ed.; VCH: Weinheim, Germany, 1992.

interactions essential for specific packing and supramolecular aggregation.

Acknowledgment. Grants to M.N.S. of the Russian Science Support Foundation and of the Bancaixa-Universitat Jaume I Foundation (Ref P1 1B2004-19) are gratefully acknowledged. The work was supported by the INTAS (Grant 2356), Russian Foundation for Basic Research (Grant 05-03-32126), and Haldor Topsøe Foundation (to A.L.G.).

Supporting Information Available: CIF files for the structures **1**−**6** and atom labeling schemes for **2** and **3**. This material is available free of charge via the Internet at http://pubs.acs.org.

IC050962C